

Introducing a mini-catamaran to perform reflectance measurements above and below the water surface

Jean-Marie Froidefond

Département de Géologie et d'Océanographie, UMR CNRS 5805
Université Bordeaux I, Avenue des facultés, 33405 Talence cedex, France
jm.froidefond@epoc.u-bordeaux1.fr

Sylvain Ouillon

Institut de Recherche pour le Développement, UR 103
BP A5, 98848 Nouméa cedex, New Caledonia
ouillon@noumea.ird.nc

Abstract: An innovative platform is tested to perform reflectance measurements at sea. This platform is a mini-catamaran with two hulls 1m long and set 0.7m apart, fitted with optical sensors. It can be used far away from an oceanographic ship to avoid its hull influencing the measurement. Reflectance measurements were performed with a TriOS radiance sensor placed +2cm or -2cm from the water surface and a TriOS irradiance sensor. Tests were carried out in calm seas and with cloud cover. The processing to derive marine radiances from raw measurements is detailed. When the radiance sensor is above the interface, it limits the sky reflections on the targeted surface and the radiance is identical to that deduced from measurements below the surface. When the sensor is placed at +3cm above-water or higher, glint affects the measurements. The mini-catamaran shows a good ability to measure marine reflectance with an adapted measurement protocol. Except for very turbid waters, it seems preferable to perform upwelling radiance measurements below the surface.

© 2005 Optical Society of America

OCIS code: (010.0010) Atmospheric and ocean optics

References and links

1. N.G. Jerlov, *Marine optics* (Elsevier, Amsterdam, 1976).
2. A. Morel, and L. Prieur, "Analysis of variations in ocean colour," *Limn. Ocean.* **22**, 709-721 (1977).
3. H.R. Gordon, O.B. Brown, and M.M. Jacobs, "Computed relationships between the inherent and apparent optical properties of a flat, homogeneous ocean," *Appl. Opt.* **14**, 417-427 (1975).
4. J.T.O. Kirk, "Dependence of relationship between inherent and apparent optical properties of water on solar altitude," *Limnol. Ocean.* **29**, 350-356 (1984).
5. H.R. Gordon, "Dependence of the diffuse reflectance of natural waters on the Sun angle," *Limnol. Ocean.* **34**, 1484-1489 (1989).
6. A. Morel, and B. Gentili, "Diffuse reflectance of oceanic waters: its dependence on Sun angle as influenced by the molecular scattering contribution," *Appl. Opt.* **30**, 4427-4438 (1991).
7. A. Morel, and B. Gentili, "Diffuse reflectance of oceanic waters 2: Bi-directional aspects," *Appl. Optics.* **32**, 6864-6879 (1993).
8. S.Sathyendranath, L. Prieur, and A. Morel, "A three model of ocean colour and its application to remote sensing of phytoplankton pigments in coastal waters," *Int. J. Remote Sens.* **10**, 1373-1394 (1989).
9. IOCCG, *Remote Sensing of Ocean Colour in Coastal and Other Optically-Complex Waters* (IOCCG, Dartmouth, 2000).
10. F. Lahet, S. Ouillon, and P. Forget, "A three component model of ocean colour and its application in the Ebro River mouth area," *Remote Sens. Envir.* **72**, 181-190 (2000).
11. S. Ouillon, P. Forget, J.M. Froidefond, and J.J.Naudin, "Estimating suspended matter concentrations from SPOT data and from field measurements in the Rhône river plume," *MTS journal* **31**, 15-20 (1997).

12. J.E. O'Reilly, S. Maritorena, G.G. Mitchell, D.A. Siegel, K.L. Carder, S.A. Garver, M. Kahru, and C. McClain, "Ocean color algorithms for SeaWiFS," *J. Geoph. Res.* **103**, 24937-24953 (1998).
13. J.M. Froidefond, P. Castaing, and R. Prud'homme, "Monitoring suspended particulate matter fluxes and patterns with the AVHRR/NOAA-11 satellite. "Application to the Bay of Biscay," *Deep-Sea Res.* **46**, 2029-2055 (1999)
14. J.M. Froidefond, S. Lavender, P. Laborde, A. Herbland, and V. Lafon, "SeaWiFS data interpretation in a coastal area in the Bay of Biscay," *Int. J. Remote Sens.* **23**, 881-904 (2002).
15. H.R. Gordon, R.C. Smith, J.R.V. Zaneveld, "Introduction to ocean optics," in *Ocean Optics VII*, M.A. Blizard, ed., Proc. SPIE **489**, 2-41 (1984)
16. C.D. Mobley, "Estimation of the remote-sensing reflectance from above-surface measurements," *Appl. Optics* **38**, 7442-7455 (1999).
17. A. Morel, and B. Gentili, "Diffuse reflectance of oceanic waters 3: Implication of bidirectionality for the remote-sensing problem," *Appl. Opt.* **35**, 4850-4862 (1996).
18. A. Morel, "In-water and remote measurements of ocean colour," *Bound. Layer Met.* **18**, 177-201 (1980).
19. G.C. Chang, T.D. Dickey, C.D. Mobley, E. Boss, and W.S. Pegau. "Toward closure of upwelling radiance in coastal waters," *Appl. Opt.* **42**, 1574-1582 (2003).
20. H.R. Gordon, and A. Morel, *Remote assessment of ocean color for interpretation of satellite visible imagery: a review* (Springer-Verlag, Berlin, 1983).
21. S.B. Hooker, and A. Morel, "Platform and Environmental effects on above-water determinations of water-leaving radiances," *J. Atm. Ocean. Technol.* **20**, 187-205 (2003).
22. H. Etcheber, "Comparaison de diverses méthodes d'évaluation des teneurs en matières en suspension et en carbone organique particulaire des eaux marines du plateau continental aquitain," *J. Rech. Oceanogr.* **6**, 37-42 (1981).
23. C.S. Yentsch, and D.W. Menzel, "A method for the determination of phytoplankton chlorophyll and pheophytin by fluorescence," *Deep-Sea Res.* **10**, 221-231 (1963).
24. D. Doxaran, R.C. Nagur Cherukuru, and S.J. Lavender, "Estimation of surface reflection effects on upwelling radiance field measurements in turbid waters," *J. Optics A: Pure Appl. Opt.* **6**, 690-697 (2004).
25. T. Ohde, and H. Siegel, "Derivation of immersion factors for the hyperspectral TriOS radiance sensor," *J. Opt. A: Pure Appl. Opt.* **5**, L12-L14 (2003).
26. S. Tassan, "Evaluation of the potential of the Thematic Mapper for marine application," *Int. J Remote Sens.* **8**, 1455-1478 (1987).
27. S. Khorram, H. Cheshire, A.L. Geraci, and G. La Rosa, "Water quality mapping of Augusta Bay, Italy from Landsat-TM data," *Int. J. Remote Sens.* **12**, 803-808 (1991).
28. S. Ouillon, P. Douillet, and S. Andréfouët, "Coupling satellite data with in situ measurements and numerical modeling to study fine suspended sediment transport: a study for the lagoon of New Caledonia," *Coral Reefs* **23**, 109-122 (2004).
29. D. Doxaran, J.M. Froidefond, P. Castaing, "Remote sensing reflectance of turbid sediment-dominated waters. Reduction of sediment type variations and changing illumination conditions effects by use of reflectance ratios," *Appl. Opt.* **42**, 2623-2634 (2003).

1. Introduction

One main application of remote sensing to coastal oceanography is to determine and quantify the particulate and dissolved matter in the surface marine waters. The key parameter in marine optics is reflectance, defined by [1-2]:

$$R(\lambda, z) = E_u(\lambda, z) / E_d(\lambda, z) \quad (1)$$

where λ is the wavelength, z is the depth from the air-sea interface, E_u is upwelling irradiance and E_d is downwelling irradiance. The reflectance at a depth $z=0^-$ is "just below the surface" and the reflectance at $z=0^+$ is "just above the surface". $E_u(\lambda, 0^-)$ is generally extrapolated from the measurement of $E_u(\lambda, z)$ according to Beer's law:

$$E_u(\lambda, 0^-) = E_u(\lambda, z) / e^{-[K_u(\lambda), z]} \quad (2)$$

where $K_u(\lambda)$ is the diffuse attenuation coefficient for upwelling irradiance.

Reflectance is also expressed using inherent optical properties of the water mass which, using a first-order model for a homogeneous ocean, gives [3]:

$$R(\lambda) = f \cdot [b_b(\lambda) / (a(\lambda) + b_b(\lambda))] \quad (3)$$

where factor f depends on the illumination conditions [4-5] and on the water optical properties [6-7]. Global absorption (a) and backscattering (b_b) result from the sum of the optical

contributions related to "pure" seawater (w index), to phytoplankton (ch index), to mineral particles (s index) and to coloured dissolved organic matter (CDOM) (y index), as follows [8-9]:

$$a(\lambda) = a_w(\lambda) + a_{ch}(\lambda) + a_s(\lambda) + a_y(\lambda) \quad (4)$$

$$b_b(\lambda) = b_{b_w}(\lambda) + b_{b_{ch}}(\lambda) + b_{b_s}(\lambda) \quad (5)$$

a_{ch} , $b_{b_{ch}}$, a_s and b_{b_s} can be expressed using the specific absorption or backscattering coefficients multiplied by the concentration in chlorophyll-a or in mineral particulate matter. Reflectance can thus be used, via an inversion method, to determine the concentrations of the various constituents (e.g., Ref. [10]). However, as it is difficult to measure all the specific coefficients accurately, an empirical approach is also used to study the variations in reflectance according to the concentrations in particulate matter or in chlorophyll pigments [11-14].

For remote sensing applications, remote-sensing reflectance (Rrs) is also used [9; 15-16]:

$$Rrs(\lambda, \theta, \phi) = Lw(\lambda, \theta, \phi, 0^+) / Ed(\lambda, 0^+) \quad (6)$$

where Lw is upwelling radiance coming from the sea – which excludes the reflected rays on the surface which have not penetrated the water –, θ is the zenith angle of the measurement, and ϕ is the azimuth. For the sake of simplification, the angles θ and ϕ will not be mentioned hereafter. Our measurements are made at the nadir ($\theta = 0^\circ$). $Rrs(\lambda)$ can be deduced from spatial radiance measurements or from measurements at sea. The name of this parameter, which was originally designed for spatial applications, is also used for optical measurements at sea. $R(\lambda, 0^+)$ and $Rrs(\lambda)$ differ by a proportionality factor Q which is a function of the directionality of the light and the optical properties of the water [7; 17].

To obtain $Rrs(\lambda)$, irradiance $Ed(\lambda)$ can be measured directly using an instrument, but this is not the case with $Lw(\lambda)$. When radiance is measured above-water, the signal from the water is contaminated, particularly by the surface reflections, and when radiance is measured below the surface it is necessary to use some hypotheses in order to deduce $Lw(\lambda)$. This calculation takes account of both the variation in solid angle between the submerged and emerged measurements caused by the variation in the refraction index, and the transmission of the signal to the water-air interface, reduced by Fresnel reflectance. If n is the refraction index of water in relation to the air and t is radiance transmittance at the water-air interface, we obtain [18-19]:

$$Lw(\lambda) = t/n^2 * Lu(\lambda, 0^-) \quad (7)$$

If we adopt $n=1.34$ for seawater [20] and $t=0.98$ for a sensor pointing towards the nadir [19], proportionality factor t/n^2 has a value of 0.546 [21]. Chang et al. [19] recommend measuring $Lu(\lambda)$ at different depths, extrapolating up to the surface using Beer's law in order to obtain $Lu(\lambda, 0^-)$, then deducing $Lw(\lambda)$ by Eq. 7.

To avoid making underwater profiles of $Lu(\lambda, z)$, we built a structure enabling measurements of upwelling radiance that are very close to the interface. This structure is a mini-catamaran fitted with an irradiance sensor placed above the water surface and pointing vertically up towards the sky, and a radiance sensor above or below the water surface, pointing vertically towards the water. It was designed to limit its own influence and that of the hull of the oceanographic ship on the optical measurement. This article presents test-measurements performed with the prototype of this catamaran with a covered sky. The first part of the article presents the equipment and protocol used. The second part presents the results obtained with the radiance sensor placed above and below the water surface in a natural environment (Bay of Arcachon, France) and compares the radiance and irradiance measurements, and the resulting reflectances. The third part is a discussion on the results and on possible developments of this new platform.

2. Measuring equipment and method

2.1 Instrument and platform

Measurements were taken with a TriOS spectroradiometer (www.TriOS.de) comprising an irradiance sensor (Ramses n°8108 ACC) and a radiance sensor (Ramses n°8091 ARC), wavelength and energy calibrated, simultaneously performing measurements with a step of 5nm between 350nm and 950nm. The calibration of the two sensors was checked before and after our field campaign using a portable calibration device (FieldCal) developed by TriOS gmbH and by G.M. Regeling and M.R. Wernand of the Netherlands Institute for Sea Research (NIOZ). This device uses a super bright white LED as the light source placed in a black, non-reflective cylinder which fits exactly to the sensors. The calibration spectra recorded on 1st March 2003 and 20 March 2004, before and after the field measurements shows an average drift < 0.6 % in the range 425-800 nm of significant light emission (Fig. 1).

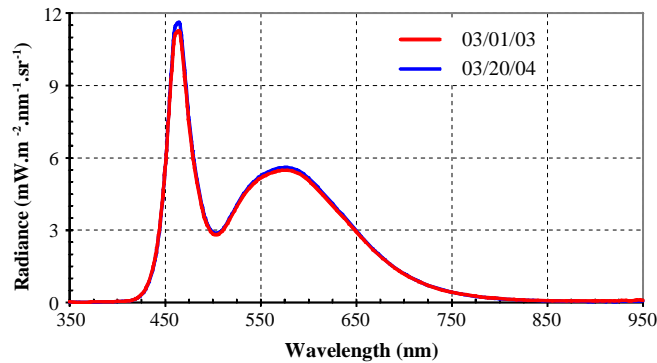


Fig. 1. Calibration radiance spectra measured using the FieldCal device.

These sensors were mounted on an easily-transportable mini-catamaran that we developed. It has two hulls 1m long, 0.25m wide and 0.15m high, made of plywood 3mm thick, joined together by two arms 0.7m long. The sensors are in the middle of these arms and are fixed to a vertical bracket (Fig. 2). The dimensions of this mini-catamaran were chosen in order to reduce its influence on the optical measurements and to enable measurement far from an oceanographic ships. The first prototype, used in this study, was not profiled to be towed. Its weight is 8Kg, and 10Kg with the sensors.

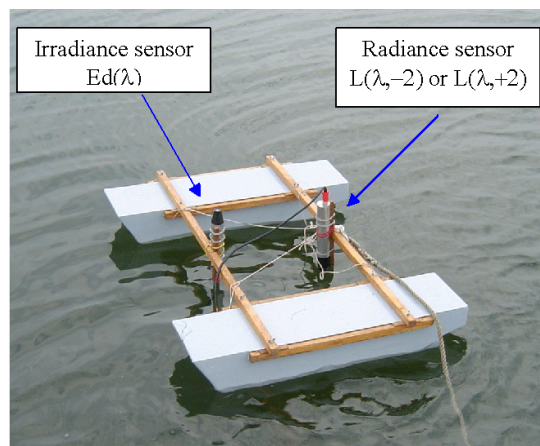


Fig. 2. Measurement platform fitted with TriOS irradiance and radiance sensors.

2.2 Measurement protocol

The irradiance sensor ($E_d(\lambda,0^+)$) points towards the zenith and performs a measurement simultaneously with each radiance measurement. We adopted the following protocol:

- 1) positioning of the objective of the radiance sensor pointing towards the nadir +2cm above the surface (± 1 cm according to the lap of the water); the corresponding measurement is noted $L(\lambda,+2)$,
- 2) at least 10 measurements carried out with a time step of 10 seconds between each measurement,
- 3) positioning of the objective of the radiance sensor pointing towards the nadir -2cm (± 1 cm) below the water surface; the measurement is noted $L(\lambda,-2)$,
- 4) at least 10 measurements carried out with a time step of 10 seconds,
- 5) one litre of surface water sampled near the sensors to measure the total suspended matter concentration by filtration (diameter $> 0.7 \mu\text{m}$) and the chlorophyll-a concentration by fluorescence. The measurements of suspended particulate matter were taken with Whatman @ GF/F filters with a diameter of 4.9mm and porosity of $\approx 0.7 \mu\text{m}$. The filters were rinsed with a solution of ammonium formate following the method of Etcheber [22]. For chlorophyll-a and phaeopigment determinations, 0.5 L of seawater was filtered through Whatman GF/F filters and immediately frozen (-20°C) until further analysis using the fluorimetric method of Yentsh & Menzel [23], with a calibrated Turner Design 700 fluorometer.

This protocol was tested in a laboratory with the radiance sensor distances reduced to +1cm and -1cm from the interface, by placing an aquarium on a white reflectance Spectralon® plate (0.31m \times 0.31m) by Labsphere (standard SRT-99-120) (Fig. 3). The two resulting spectral radiances are similar (Fig. 4). The deviation observed (2.1% in average from 400 to 700nm) is likely due to three factors: the correction to convert the raw underwater measurement into equivalent above-water radiance, the light absorption in the first centimetre under the surface, and the glint in the above-water measurement. This small deviation is analysed later.

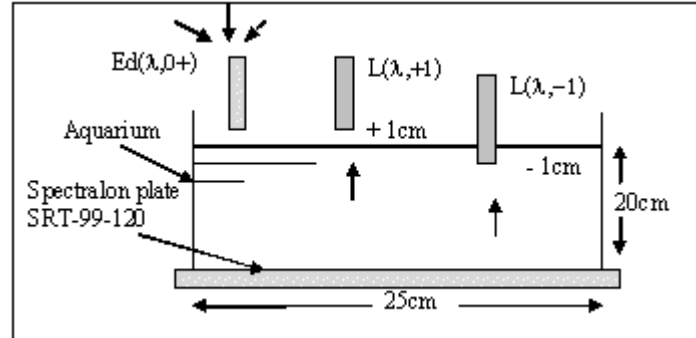


Fig. 3. Testing device comprised of an aquarium placed on a white reflectance Spectralon® plate and in the shade to avoid major reflections on the glass tank.

In the natural environment, the measurements were performed at 13 stations in the Bay of Arcachon on 17 and 18 February 2004 with a calm sea or slight lapping, and a uniformly covered sky. The Bay of Arcachon is located 50km west of Bordeaux (France). It is a semi-enclosed Bay of 11km \times 11km, and two-thirds of its area is emerged at low tide. The measurements were carried out in channels of the Bay at high tide. Stations considered in this study were such that the Secchi disk depth was less than the water depth so as to insure against the bottom influence on surface reflectance. The mini-catamaran was launched at each station around 15 metres away from a small oceanographic ship.

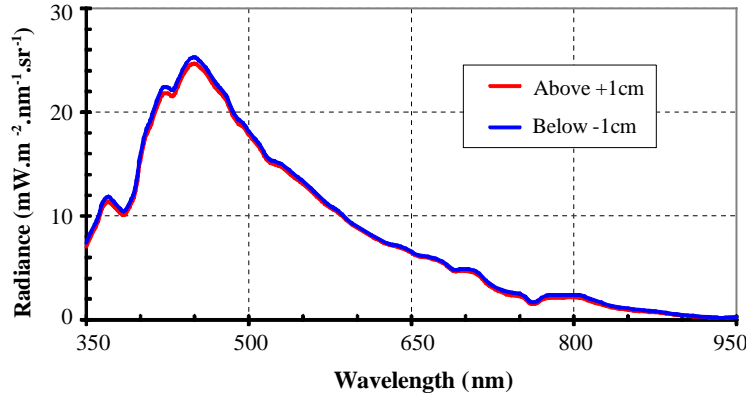


Fig. 4. Spectral radiances obtained following the schema of Fig. 3. The below-water spectrum $L(\lambda, -1)$ corresponds to a non-corrected radiance.

2.3 Correction of radiances and calculation of remote-sensing reflectance

The radiance measured above-water $L_t(\lambda)$ can be expanded as [21]:

$$L_t(\lambda, 0^+) = L_w(\lambda) + \rho L_{\text{sky}}(\lambda) + \Delta L_{\text{ship}}(\lambda) \quad (8)$$

where ρ is the Fresnel reflectance of the air-water interface, $L_{\text{sky}}(\lambda)$ the sky radiance and $\Delta L_{\text{ship}}(\lambda)$ the radiance from solar reflection on the hull of the ship which re-crossed the surface towards the sensor. The glint is generally high in above-water measurements [24]. However, when the TriOS sensor is placed just above-water, it limits the sky reflections on the small targeted area. Finally, the distancing of the platform from the oceanographic ship considerably reduces the reflections of the immersed structures nearby, which here are limited to the small catamaran.

As the TriOS spectroradiometer was calibrated for measurements in the air [25], the variation in the index of refraction between the air and the water modifies the opening angle of the radiance measurement. In the air, the semi-opening angle was 3.5° . In seawater, the corresponding value is given by the law of Descartes according to:

$$\theta_{\text{water}} = \arcsin [(1/n) * \sin\theta_{\text{air}}] \quad (9)$$

which gives a semi-opening $\theta_{\text{water}} = 2.611^\circ$ with $n = 1.34$. The solid angle Ω_{IFOV} of semi-opening angle θ is, in steradians:

$$\Omega_{\text{IFOV}} = 2 \pi (1 - \cos\theta) \quad (10)$$

The solid angle of measurement is thus $11.719 \cdot 10^{-3}$ sr in the air and $6.524 \cdot 10^{-3}$ sr in the water. Therefore, this solid angle corresponding to the measurement is 1.796 times greater in the air than in the water. This factor multiplied by the raw measurement performed at 0^- gives $L_u(\lambda, 0^-)$. It is called the correction factor or the immersion factor, and is noted F . The value 1.796 is close to the values given by Ohde and Siegel [25] for the TriOS radiance sensor. Ohde and Siegel calculated the theoretical spectral values of F from the spectral indices of the seawater and the glass window of the sensor on one hand, and obtained experimental values of F by comparing the measurements made by the TriOS sensor and by a Satlantic sensor commonly used in marine optics on the other hand. They obtained a theoretical F factor gradually varying between 1.774 at 350nm and 1.722 at 950nm, and a variable experimental factor with the wavelength, between 1.654 and 1.972. The value that we deduced from the opening angle of the sensor and the index of refraction of the seawater, $F = 1.796$, is consistent with their results.

The raw (i.e. uncorrected) upwelling radiance measured below-water, $L(\lambda,-2)$, must be multiplied by F to obtain $L_u(\lambda,0^-)$, and by a global factor $F \cdot t/n^2$ (Eq. 7), i.e. $1.796 \cdot 0.546 = 0.98$, to obtain $L_w(\lambda)$:

$$L_w(\lambda) = 0.98 \cdot L(\lambda,-2) \quad (11)$$

When remote-sensing reflectance R_{rs} is deduced from the measurement of $L(\lambda,-2)$ rather than an above-water radiance measurement, it is calculated by the following combination of Eq. 6 and 11:

$$R_{rs}(\lambda) = 0.98 \cdot L(\lambda,-2) / E_d(\lambda,0^+) \quad (12)$$

3. Results

3.1 Irradiance and radiance

Two typical examples of measurements taken above and below the water surface at the “Aiguillon” station ($44^\circ 39' 50'' N$, $1^\circ 08' 45'' W$) on 17 February 2004, between 10:44 am and 10:52 am local time, and at the “Teychan” station ($44^\circ 40' 278'' N - 1^\circ 10' 498'' W$) on 18 February 2004 between 9:16 am and 9:30 am, under a uniformly cloudy sky, are illustrated in Fig. 5, 6 and 7. As the results obtained for the 12 other stations do not differ in principle, they are not detailed in the paper.

Two series of spectral irradiance ($E_d(\lambda,0^+)$) were measured at Aiguillon with a 6-min lag (Fig. 5). The corresponding two series of upwelling radiance measurements were performed on either side of the water surface (Fig. 6). The uncorrected spectral radiance measured under the surface is more reproducible than the luminance measured above-water (Fig. 6).

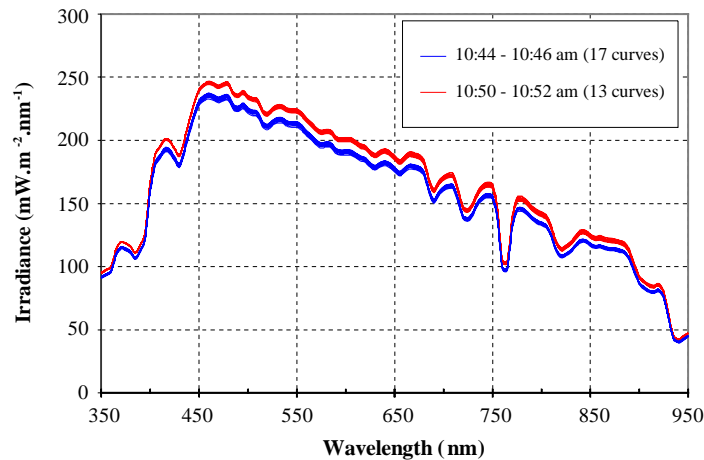


Fig. 5. Irradiance measured at Aiguillon under a covered sky on 17 February 2004 between 10:44 and 10:46 am and between 10:50 and 10:52 am.

The test carried out at Teychan consisted of measuring the above-water radiance with the sensor a little further away from the interface (+3cm). The corresponding radiances are strongly higher than the uncorrected radiances measured under the surface (Fig. 7). This phenomenon can be accounted for by the glint, which is minor when the sensor is +2cm away (Fig. 6) and much greater when the sensor does not mask the skylight reflections on the interface (Fig. 7). $\rho_{L_{sky}}(\lambda)$ is thus higher than $L_w(\lambda)$ in the above-water measurement of radiance (see Eq. 8).

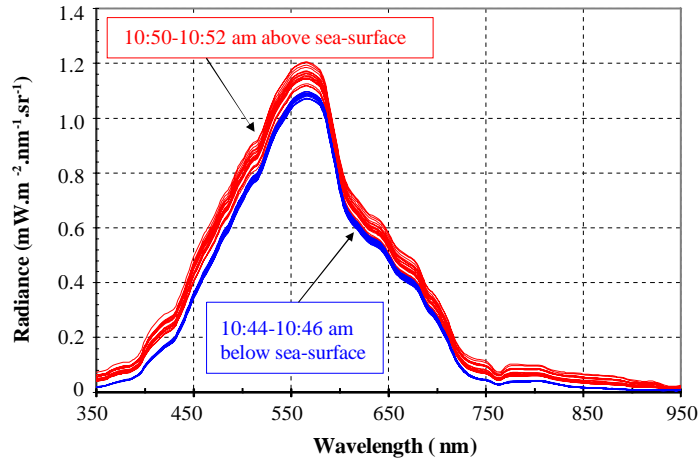


Fig. 6. Upwelling radiance measured at $+2\text{cm} \pm 1\text{cm}$ (17 red curves) and at $-2\text{cm} \pm 1\text{cm}$ (13 blue curves, uncorrected radiance) simultaneously with an irradiance measurement presented in Fig. 5. Aiguillon, 17 February 2004.

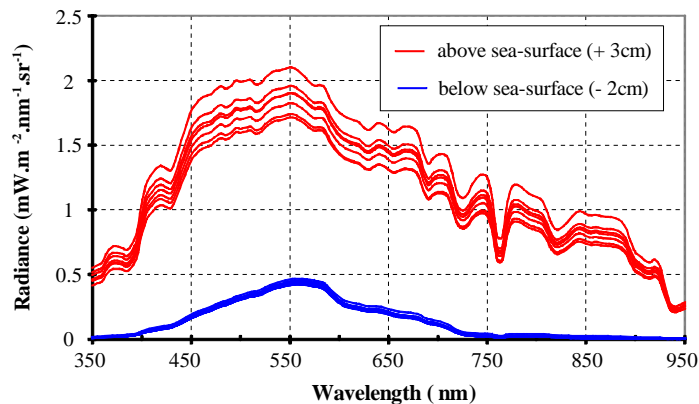


Fig. 7. Radiance measured above-water at $+3\text{cm}$ (7 red curves) and below the sea surface at -2cm (33 blue curves, uncorrected measurements), Teychan, 18 February 2004.

3.2 Remote-sensing reflectance

The remote-sensing reflectance spectra at Aiguillon correspond to a concentration in Total Suspended Matter (TSM) of 1.58 mg/L and a concentration in chlorophyll-*a* of 0.44 mg/m^3 (Fig. 8). The shape of these spectra is typical of coastal waters of this region [14]. The spectra from underwater measurements present a lower standard deviation (SD, between $5 \cdot 10^{-5}$ and $7 \cdot 10^{-5}$) than those measured above-water (SD between 10^{-4} and $1.5 \cdot 10^{-4}$). The difference between the average values of R_{rs} obtained from the measurements above and below the surface is high in the near ultraviolet and the near infrared ($>100\%$) because the water radiance is low at these wavelengths. Around the peak of R_{rs} (Fig. 8), between 550 and 600nm, the difference between the average spectra calculated from measurements above and below the surface is less than 4 %.

Adopting this method, we obtained 10 to 15 remote-sensing reflectance spectra from the measurements carried out at -2cm per station, on several stations. These spectra present a standard deviation lower than or equal to 10^{-4} for a given station. The average spectrum was calculated for each station. The average spectra for 7 stations are presented in Fig. 9 with the corresponding TSM and chlorophyll-*a* concentrations. The accuracy of the measurements

allows us to distinguish water presenting a TSM difference lower than 1 mg/L. Reflectance between 500nm and 700nm increases significantly with the TSM concentration, in accordance with previous works [11;13]. The reflectance peak is situated at 575nm. Regarding chlorophyll-a, the relatively low concentrations, between 0.38 mg/m³ and 1.18 mg/m³, were compared with the ratios Rrs440/Rrs555 and Rrs490/Rrs555, often used in chlorophyll quantification algorithms (*e.g.*, Ref. 12). These ratios present reduced ranges: 0.20-0.37 for Rrs440/Rrs555 and 0.48-0.65 for Rrs490/Rrs555. They do not decrease consistently with the chlorophyll-a concentrations. Indeed, the Bay of Arcachon waters are case 2 waters with a high TSM concentration (> 1mg/L) for which Rrs440/Rrs555 and Rrs490/Rrs555 are highly dependent on the terrigenous particulate matter content [14].

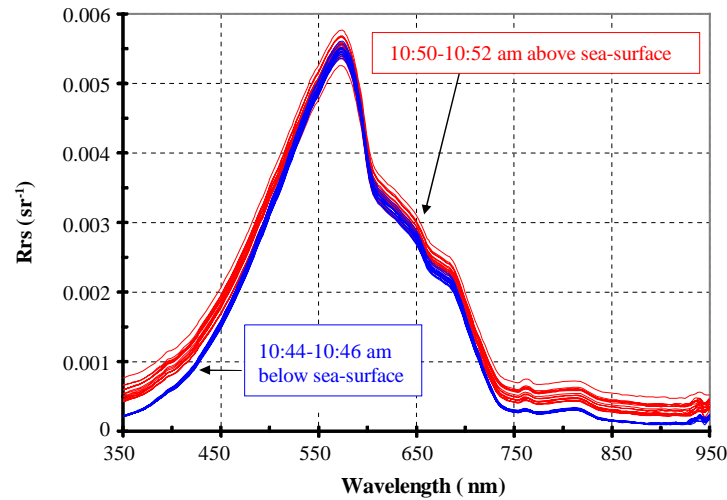


Fig. 8. Remote-sensing reflectance calculated from irradiance and radiance shown in Fig. 5 and 6 at Aiguillon on 17 February 2004: $Rrs = Lw/Ed$ with Lw computed from $Lu(-2)$ in blue (measurements taken between 10:44 am and 10:46 am) and $Rrs = L(+2)/Ed$ in red, measurements taken between 10:50 am and 10:52 am).

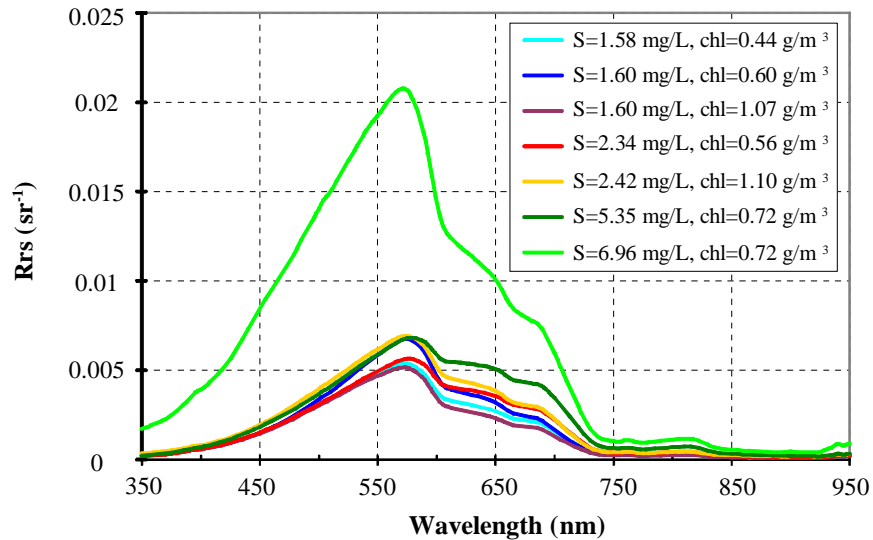


Fig. 9. Remote-sensing reflectance and corresponding concentrations in Total Suspended Matter (S) and in chlorophyll-a (chl) for 7 stations in the Bay of Arcachon, 17 and 18 February 2004.

4. Discussion

The first comment concerns the small difference between the uncorrected radiance measurements performed just above and just below the water surface (Fig. 6). This may seem surprising because the indices of refraction of air and water are different. But whether these measurements are taken above or below the surface, the light rays coming up from the water column go to the air through the glass of the objective, with the photodiodes always in the air, even when the radiance sensor is submerged. The change in index of refraction does therefore not occur on the level of the energy received. However, although similar, the in-water and above-water uncorrected radiances are not equal. The sensor calibration carried out in the air by the manufacturer (TriOS) enables the direct conversion of the above-water measurements into radiance $Lu(0^+)$. For in-water measurements, this conversion must be subject to a correction, either to obtain $Lu(0^-)$ or to obtain $Lw(0^+)$. The multiplying factor to be applied is 1.796 to obtain $Lu(0^-)$ and 0.98 to obtain $Lw(0^+)$. Factor 0.98 takes account of the loss of signal at the passage through the air-water interface (Fresnel reflectance) which causes the difference of 2.1% between the raw radiance measurements carried out in an aquarium (paragraph 2.2, Fig. 4), which shows, in this case, that light absorption in the first centimetre below the surface and the reflections in the above-water measurement did not introduce a significant bias into the measurement.

The major result of this work concerns the consistency of the reflectance values calculated from the measurements taken just above and just below the interface (Fig. 8), thanks both to the prototype and to the measurement protocol. Rrs values differed by less than 4% in the spectral region of maximum reflectance depending on whether they were calculated from measurements above or below the water surface. The absolute difference between Rrs values did not exceed 0.0005 sr^{-1} in our tests. Relative deviations are higher in the near ultraviolet and in the near infrared because reflectance is very weak in these spectral regions. This measurement accuracy is sufficient to establish the TSM quantification algorithms based on reflectance in the 550-600 nm range, which is, for example, the case of algorithms built for Landsat TM band 2 (e.g., Ref. 26-28). It should be noted that large deviations in the near infrared apply to reflectances, but that reflectance ratios, often used in this range for very turbid waters [29], present much smaller deviations.

The good consistency of the Rrs values derived from measurements above and below the surface shows that the experimental prototype, when the radiance sensor is just above the surface, gives remote-sensing reflectance from a simple ratio of radiance and irradiance measurements without need to correct the optical influence of the hull (Eq. 8). This frequently observed effect causes uncertainty in the processing of data, an uncertainty which disappears when a very small measurement platform is used. However, we have shown with one example (Fig. 7) to what extent the measurement can be distorted by the glint when the sensor is not targeting its own shadow. We cannot assimilate the values of $L_r(0^+)$ measured with $Lw(0^+)$ when the sensor does not mask the reflection of the sky on the targeted surface. The corresponding surface-effect correction can be made with certain hypotheses [16] as long as it is also possible to measure L_{sky} (Eq. 8). This correction nonetheless remains difficult because $Lw(0^+)$ can represent less than 50% of $L_r(0^+)$ out of the spectrum as a whole (Fig. 7), as Doxaran et al. [24] have also shown.

When the objective of the radiance sensor is submerged, the light attenuation by the water in the $2\text{cm} \pm 1\text{cm}$ surface layer can introduce a bias in relation to the measurement which could be made just below the interface (at 0^-). This attenuation depends on the particulate and dissolved matter present in the water. In order to fix its order of magnitude in an example, the diffuse attenuation coefficient K_d was deduced from $Ed(z)$ measurements for a station more turbid than Aiguillon (6.96 mg/L of mineral particulate matter instead of 1.58 mg/L), on 17 February 2004, using the relation:

$$Ed(\lambda, z) = Ed(\lambda, 0^-) \cdot e^{-[K_d(\lambda) \cdot z]} \quad (13)$$

The resulting K_d varied between 1.55m^{-1} (at 400 and 700nm) and 0.74m^{-1} , with the minimum value reached at 570nm. By introducing these values into equation 13, the incident solar irradiance at -2cm is 98.5 % of the surface irradiance at 570nm, and 97% of this same irradiance at 400nm or 700nm. In more turbid water, K_d reaches higher values and light at -2cm is greatly attenuated compared to the surface. The particulate load also attenuates upwelling radiance. For water with a very high mineral concentration (estuaries, for example), given the attenuation, it will be preferable to perform measurements above-water in order to obtain remote-sensing reflectance. The tested mini-catamaran allows such measurements to be taken.

5. Conclusion

In order to carry out reflectance measurements just above or just below the water surface, an easily transportable mini-catamaran was made in plywood in order to use a TriOS spectroradiometer. The results show that the radiance spectra measured in average turbid waters (between 1 and 7 mg/L approximately) with the objective +2cm above and -2cm below the surface enable the calculation of two close R_{rs} values in the 550-600 nm range (difference < 4%). However, we show that measurements of upwelling radiance at the nadir, 3cm above the water, that were not carried out in the area of limited sky reflections by the sensor are strongly disturbed by the glint, which is difficult to correct. It seems thus preferable to perform in-water measurements of upwelling radiance, except in very turbid waters where the light attenuation significantly modifies irradiance and radiance in the first centimetres below the surface. The tested structure shows a good ability for reflectance measurement at sea, above or below the surface, using an adapted measurement protocol. Further tests in very turbid water ($SPM > 10 \text{ mg/L}$) will have to be carried out. On the basis of the trials presented in this paper, variants could be tested in the measurement protocol and the overall procedure could be attempted under different measuring conditions (clear sky, presence of waves). It is not, for example, necessary for the incident solar irradiance to be measured from the mini-catamaran. This can be done nearby, with the sensor maintained vertically, which should limit the variation in measurements in the presence of waves (variable orientation of the sensor), and this is not the case of the measurements presented in this article. Another variant in the protocol consists of measuring the above-water radiances not at the nadir but with a tilt of around 40° from vertical (e.g., Ref. 16) in order to minimise the reflections on the measurement zone using the mini-catamaran.

Acknowledgments

This work was supported by the French programmes “ACI Observation de la Terre” and “PNEC-Littoral Atlantique”. We warmly thank Corine Glé who performed the chlorophyll concentrations and the crew of the R.V. *Planula-III* from the “Laboratoire d’Océanographie Biologique” of Arcachon (UMR CNRS 5805), and the Association “Voile d’Antan” (Gujan-Mestras, France).